diversity

MDPI

Article

Spatiotemporal Distribution and Dispersal Pattern of Early Life Stages of the Small Yellow Croaker (*Larimichthys Polyactis*) in the Southern Yellow Sea

Xiaojing Song [1,2], Fen Hu [1,2], Min Xu [1,2], Yi Zhang [1,2], Yan Jin [1,2], Xiaodi Gao [1,2], Zunlei Liu [1,2,*], Jianzhong Ling [1,2], Shengfa Li [1,2] and Jiahua Cheng [1,2,*]

[1] East China Sea Fisheries Research Institute, Chinese Academy of Fishery Sciences, Shanghai 200090, China; songxiaojing@ecsf.ac.cn (X.S.); hufen518@sohu.com (F.H.); xuminwzy@aliyun.com (M.X.); zhangyiyutianx@163.com (Y.Z.); jenniferyanjin@163.com (Y.J.); xd_gao@foxmail.com (X.G.); lingjianzhong18@sina.com (J.L.); lisf@ecsf.ac.cn (S.L.)

[2] Key Laboratory of East China Sea Fishery Resources Exploitation and Utilization, Ministry of Agriculture and Rural Affairs, Shanghai 200090, China

* Correspondence: liuzl@ecsf.ac.cn (Z.L.); dhsziyuan@163.com (J.C.)

Abstract: Nursery habitats play a significant role in completing fish life cycles, and they are now recognized as essential habitats. Monthly variations in nursery ground distributions of *Larimichthys polyactis* were investigated in the southern Yellow Sea in 2019. Bayesian hierarchical models with integrated nested Laplace approximation were utilized to model the preferential nursery habitats of *L. polyactis* larvae. The study analyzed the spatial and temporal distributions of the larvae and juveniles based on three environmental variables: sea surface temperature, sea surface salinity, and depth. Additionally, this study examined the utilization of habitats by different fish life stages and ontogenetic shifts. A total of 3240 individuals were collected from April to June, with the peak occurring in May (0.05 ind./m^3), and the distribution areas varied between different months. The prediction of the model reveals the ecological adaptability of *L. polyactis* to temperature variations. The optimal temperature for *L. polyactis* density ranges from 12.5 °C to 16.5 °C in April and 16.5 °C to 17.5 °C in May, demonstrating a broad temperature tolerance for *L. polyactis* survival. In addition, there are variations in distribution patterns among different developmental stages. *Larimichthys polyactis* spawn in the inshore and nearshore waters, and after hatching, larvae in the pre-flexion stage tend to remain aggregated near the spawning beds. However, larvae in the advanced development stage (post-flexion) and juveniles move towards the sandy ridge habitats along the coast and start to migrate offshore in June. This study provides valuable insights for the effective management of fishery resources in the area and can be utilized to identify marine areas with specific habitat features that require conservation.

Keywords: sdmTMB; larvae and juveniles; nursery ground; ontogenetic habitat shifts; coastal waters

Citation: Song, X.; Hu, F.; Xu, M.; Zhang, Y.; Jin, Y.; Gao, X.; Liu, Z.; Ling, J.; Li, S.; Cheng, J. Spatiotemporal Distribution and Dispersal Pattern of Early Life Stages of the Small Yellow Croaker (*Larimichthys Polyactis*) in the Southern Yellow Sea. *Diversity* **2024**, *16*, 521. https://doi.org/10.3390/d16090521

Academic Editor: Bert W. Hoeksema

Received: 24 July 2024
Revised: 27 August 2024
Accepted: 28 August 2024
Published: 31 August 2024

1. Introduction

The population dynamics of many fish species are greatly influenced by fluctuations in their early life stages, including the egg, larval, and juvenile periods [1], because early life stages are particularly vulnerable, with mortality rates of up to 99% recorded for marine species [2]. Some habitats may provide better conditions for larvae and juveniles, especially favoring survival, as is the case of estuaries and shallow coastal areas. Therefore, the study of early life history, encompassing distribution, dispersal, and survival, has been a prominent topic in fishery oceanography. Hydrological conditions are critical variables influencing the selection of fish spawning sites and the survival of larvae [3]. Various hydrological recruitment hypotheses have been suggested, including the match–mismatch hypothesis, ocean triads, and stable ocean hypothesis [4]. Studies investigating

the early distribution of fish have uncovered a tendency for fish spawning and nursery grounds to concentrate in close proximity to oceanic fronts [5,6]. This indicates that the presence of fronts generates specialized habitats through physicochemical processes [7]. The distribution of larvae in nutrient-rich regions results from upwelling currents and tidal mixing, the concentration of larvae in areas of convergence or fronts, and the existence of drift retention areas.

The small yellow croaker, *Larimichthys polyactis* (Bleeker, 1877), is a warm-temperate fish of Acanthuriformes (Sciaenidae), mainly inhabiting estuaries and coastal waters [8]. It is a typically migratory species widely distributed in the Bohai Sea, Yellow Sea and East China Sea of the Northwest Pacific [9,10]. This particular species holds great economic significance in China, with a long history of fishing and contributing over 300 thousand tons of fishery yield annually to both China and South Korea. Nevertheless, the population of *L. polyactis* has been at risk of declining genetic diversity and abundance in recent years because of overfishing and environmental changes [11,12]. Genetic diversity losses are characterized by earlier sexual maturity, smaller fish sizes, and a growing predominance of young fish [13]. Specifically, older females usually produce disproportionally more eggs relative to younger and smaller individuals [4]. Higher-quality offspring, produced by older females, might be more likely to survive, as they can experience lower mortality rates when facing poor habitat quality [14]. As young fish continue to dominate the spawning stocks, the early life stage survival becomes of increasing concern, and preserving essential fish habitats during early life history stages might serve as an important approach for resource recovery [15–17].

The coastal waters of the southern Yellow Sea are considered as the largest spawning and nursery ground for *L. polyactis* in China [18]. In spring, *L. polyactis* returns to the coastal waters for spawning from open sea. It spawns pelagic eggs, and its spawning and nursing areas are usually located in estuaries, bays and radiating ridges [19]. It is known that adult females of *L. polyactis* spawn 7944~31,077 eggs that are 0.41–2.77 mm in diameter [20]. Under appropriate physiological conditions, it generally takes ~50 h for eggs to hatch after spawning followed by ~25 days for the larvae to grow to the juvenile stage [21]. The abundance of eggs and larvae was found to be related to the specific temperature and salinity characteristics of the water. Xu et al. supposed that the Changjiang River plume and its front structure could determine the distributions of the eggs and larvae [13]. In the southern Yellow Sea, the distinct hydrodynamic and tidal currents might play an important role in the transport and migratory potential during the early life stages, especially the pelagic larvae with ontogenetic variation in swimming abilities [13,22]. The coastal waters of the southern Yellow Sea are characterized by various microhabitats, such as sand ridges, plains, and bays, which reflect the diversity of aquatic habitats present (Figure 1). Ontogenetic habitat shifts during the life history play an essential ecological role. Larvae tend to drift with currents and settle in nursery areas like estuaries and coastal zones, where they can find abundant food and protection from predators. As they mature into juveniles, their requirements for space, prey, and habitat complexity often increase, leading them to migrate to different habitats [23]. Therefore, understanding stage-specific distribution patterns is imperative for conducting a detailed examination of habitat utilization and for formulating robust conservation measures.

In this study, we conducted monthly surveys of ichthyoplankton in the coastal waters of Jiangsu Province during March 2019 and January 2020. By analyzing the observed patterns of *L. polyactis* distribution in the early life stage alongside corresponding hydrological observations, we investigated the influence of hydrology on the distribution of *L. polyactis* larvae and juveniles in the coastal waters of Jiangsu. The main objectives of this study were to (1) examine the timing, locations, and hydrological characteristics of fish spawning, and (2) analyze the spatial heterogeneity of distribution to examine stage-specific patterns of habitat use and ontogenetic habitat shifts. Through our research, we aim to emphasize the importance of considering the coastal zone in early life history studies and advocate for more sensitive management approaches in regional coastal zones.

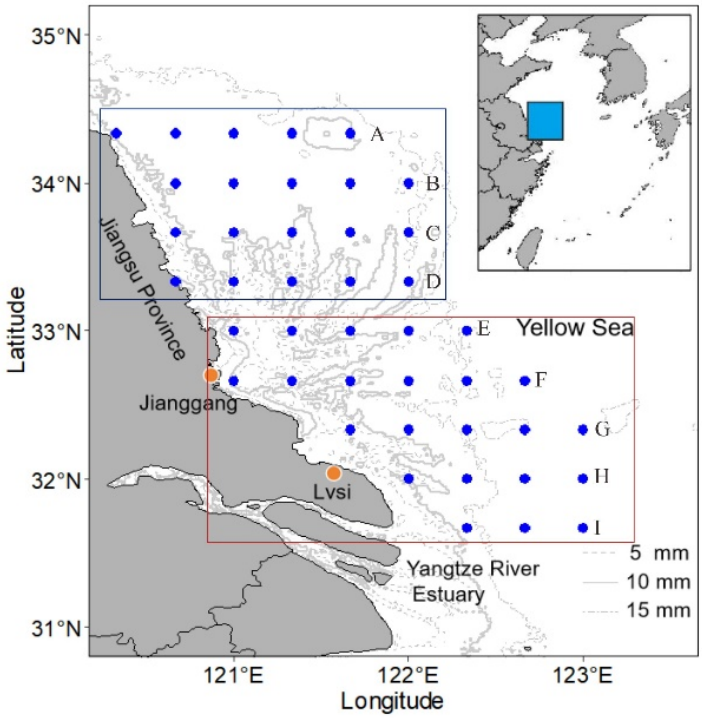

Figure 1. Schematic of the study area and sampling stations in the southern Yellow Sea. The blue rectangle is the survey area of "Huchongyu 11,050", and the red rectangle is the survey area of "Huchongyu 11,197".

2. Materials and Methods

2.1. Study Area

The study area is situated in the southern Yellow Sea of China, encompassing the entire coast of Jiangsu Province. It exhibits typical geography and hydrology characteristics. In the central region, a significant number of radiating sand ridges (RSRs) are formed due to tidal currents. Rao et al. have described an ecosystem consisting of over 70 underwater sand ridges extending from Jianggang Town, spanning 200 km north to south and 90 km east to west [24]. The water flow in the tidal channels is swift, while the sand ridges experience a gentler flow, which contributes to the development of a unique radiating sand ridge ecosystem. On the other hand, the northern region falls within the marginal area of Subei Shoal and is influenced by the coastal waters of Subei and mixed water masses from the eastern Yellow Sea. There is also freshwater input from rivers like the Guan and Sheyang Rivers. During the spring and summer seasons, this area displays a pronounced temperature thermocline in deep waters and a distinct tidal front between depths of 20 and 40 m [25]. These frontal zones are observable along the coastal and offshore regions. They have notable effects on secondary circulation, convergence, and strong mixing, which significantly impact the transport of matter, energy, and ecological processes in the ocean. Previous studies have indicated that nutrient and Chlorophyll a (Chl a) concentrations, as well as fish eggs, are higher in proximity to these frontal zones, particularly during the spring and early summer periods [26].

2.2. Data Sampling and Processing

We conducted monthly collections of ichthyoplankton in the coastal areas of Jiangsu (between 31°40′ N and 34°20′ N) from March 2019 to January 2020. These collections were carried out during the peak tidal period every month. The two fishing vessels, "Huchongyu 11,050" and "Huchongyu 11,197", possessing identical specifications and uniform physical properties, an engine power of 255 kW, and a gross tonnage of 162 tons, were assigned to specific sub-areas within the Jiangsu coastal areas. The targeted sampling encompassed 43 stations distributed across 9 cross-shelf transects, coded A to I (Figure 1).

To collect eggs and larvae, we utilized conical–cylindrical plankton nets with a mesh size of 0.5 mm and a mouth diameter of 1.3 m. To standardize the volume of filtered water, a flow meter was connected to the mouth of the net; the warp length was adjusted so that no part of the net was exposed from the surface layer. The net was dragged horizontally along the sea surface for 10 min at a constant speed of 1–2 knots. Following collection, the ichthyoplankton samples were immediately fixed and preserved in a 4% buffered seawater–formaldehyde solution. Additionally, at selected stations, a subset of up to 10 eggs and larvae was sorted from each haul and placed into individually labeled tubes containing 1.5 mL of 96% ethanol. This was carried out to facilitate identification of the eggs and larvae using DNA barcoding. At each station, vertical measurements of temperature, salinity, and depth were obtained using a Sea Bird Electronics model 19 conductivity–temperature–depth (CTD) profiler.

The ichthyoplankton samples were sorted and counted under a stereomicroscope. Eggs and fish were identified to the lowest possible taxonomic level using morphometric and meristic characteristics, based on the developmental stages described by Ahlstrom and Moser [27,28]. The primary focus of our study was the larvae, juvenile and young fish of *L. polyactis*. The larvae are divided into four stages, including yolk-sac, pre-flexion, flexion and post-flexion; the juvenile stage follows the larval stage and begins when fin ray counts are complete, and ends with the completion of squamation development; the fish enters the young period after the scales are fully grown, and the maximum body length in this paper is not more than 6 cm [29,30]. After comparing and identifying the species using DNA sequencing, we extracted the number of larvae and juveniles and the filtration water volume from the database. Larval and juvenile fish densities (ind./m^3) were estimated by dividing the abundance at a given station by the volume of water filtered. In the abundance modeling process, the density of each station was pooled together for the larvae and juveniles.

2.3. Data Analysis

2.3.1. Statistical Model

The R package sdmTMB was used to construct a spatiotemporal distribution model of *L. polyactis* in relation to environmental factors [31]. The sdmTMB utilizes the integrated nested Laplace approximation (INLA) method [32] to establish a Stochastic Partial Differential Equation (SPDE) matrix and employs the Template Model Builder (TMB) [33] to fit spatial and spatiotemporal generalized mixed models. This model extends the framework of generalized linear mixed models by incorporating two random terms in the random field: the spatial field (representing spatial processes that remain constant over time) and the spatiotemporal field (with unique spatial variations at each time point) [34]. The spatial domain effects are characterized using the Gaussian random field (GRF) method, where the random effects of spatial patterns are derived from a multivariate normal distribution (MVN) matrix constructed using the Matérn covariance function.

In the density data of *L. polyactis*, 61.2% of the values are zeros. For datasets with a high proportion of zeros or zero-inflated data, the delta method [35–37] and modeling methods that simultaneously handle zero values and positive continuous values using a single distribution (such as Tweedie) [38] are commonly employed. In this study, a spatiotemporal generalized additive mixed model (GAMM) based on the Tweedie distribution was used to model *L. polyactis* data. The Tweedie distribution is a family of exponential dispersion models that includes the power variance function $Var[y_i] = \phi\mu_i^p$, where ϕ is the dispersion parameter, μ is the mean, and p is the power parameter. When $1 < p < 2$, the distribution corresponds to a mixture of Poisson-gamma distributions and allows for zero values. The spatiotemporal GAMM for *L. polyactis* density is represented as

$$d_{\mathbf{s},m} \sim \text{Tweedie}(\mu_{\mathbf{s},m}, p, \phi),\ 1 < p < 2$$

$$\log(\mu_{\mathbf{s},m}) = \alpha_m + \sum_{i=1}^{K} f(x_i) + \omega_{\mathbf{s}} + \varepsilon_{\mathbf{s},m}$$

$$\omega_{\mathbf{s}} \sim \mathrm{MVN}(0, \Sigma_\omega)$$

$$\varepsilon_{\mathbf{s},m} \sim \mathrm{MVN}(0, \Sigma_\varepsilon)$$

The density of *L. polyactis* at station *s* in month m, denoted as $d_{(s,m)}$, is modeled using environmental covariates x_i (i = 1, …, K), where $\mu_{(s,m)}$ represents the expected value of *L. polyactis*. The environmental covariates are fitted using cubic splines, denoted as $f(\mathrm{x_i})$. The parameter α_m represents the estimated individual mean for each month. The spatial random field term is denoted as ω_s, and the spatiotemporal random field term is denoted as $\varepsilon_{(s,m)}$. The random effects (ω_s, $\varepsilon_{(s,m)}$) follow a multivariate normal distribution with a mean of 0 and a variance of the Gaussian Markov random field defined by the Matérn covariance (Σ_ω, Σ_ε) [39].

In the spatiotemporal model for *L. polyactis*, three environmental covariates were initially selected: depth (m), surface salinity, and surface temperature (°C). We did not consider the survey vessel as a fixed factor, as consistent parameters and sampling standards were maintained across all surveys. The environmental variables were standardized by subtracting their means and dividing by their standard deviations to avoid computational issues during model fitting and to allow for comparison of coefficient magnitudes [40]. sdmTMB allows for anisotropy in the spatial autocorrelation function, where spatial covariance may be asymmetric with respect to latitude and longitude, which caused spatial correlation that is directionally dependent. Anisotropy can be turned on or off with the logical anisotropy argument (anisotropy = FALSE/TRUE); we adopt a 2-parameter rotation matrix H to implement anisotropic covariance and set the default values for parameter specification. The spatiotemporal random field was set as either off or iid (spatiotemporal = "off"/"iid") [31], resulting in four candidate models (Table 1).

Table 1. Predictor covariates and specified parameters used in species distribution modeling.

Model	Covariate	Anisotropy	Spatiotemporal
M1	Month + s(depth, cs = "cc", k =4) + s(temperature, cs = "cc", k = 4) + s(salinity, cs = "cc", k = 4)	FALSE	"off"
M2	Month + s(depth, cs = "cc", k =4) + s(temperature, cs = "cc", k = 4) + s(salinity, cs = "cc", k = 4)	TRUE	"off"
M3	Month + s(depth, cs = "cc", k =4) + s(temperature, cs = "cc", k = 4) + s(salinity, cs = "cc", k = 4)	FALSE	"iid"
M4	Month + s(depth, cs = "cc", k =4) + s(temperature, cs = "cc", k = 4) + s(salinity, cs = "cc", k = 4)	TRUE	"iid"

2.3.2. Model Adequacy Diagnosis and Selection

In Bayesian hierarchical modeling, the accuracy and reliability of the model are heavily contingent upon the validity of its assumptions. If these assumptions are violated, the parameter estimates and predictions derived from the model may be unreliable. AIC offers a swift means of comparing the relative merits of competing models. However, it does not account for the validation of model assumptions. Li et al. suggested that using AIC selection should be carried out cautiously, and certainly not in isolation from other diagnostics [41]. In this paper, simulation-based residuals were calculated for all four models using the DHARMa R package [42]. Once these residuals satisfied distributional assumptions, each model was evaluated using the AIC criterion; the model with lowest AIC was used to produce maps of log(density). The residuals were simulated 3000 times for non-random effects, and the Kolmogorov–Smirnov (K-S) test was applied to test the

uniformity of the residuals. The K-S test provides a statistic (D value) and a *p*-value, where the D value measures the maximum difference between the sample residual distribution and the theoretical distribution. The p-value represents the probability of observing the D value or a more extreme value under the null hypothesis. When the D value is small and the p-value is large, it indicates a good fit of the model to the data, suggesting that the sample residual distribution is consistent with the theoretical distribution. Conversely, if the D value is large or the *p*-value is small, it indicates a significant difference between the residual distribution and the theoretical distribution, requiring a reassessment of the model fit or an examination of the data's adequacy. For the models with an insignificant residual test, AIC was used for comparison and the optimal model was selected.

3. Results

3.1. Characteristics of Depth, Temperature, and Salinity

The coastal areas of middle Jiangsu province exhibit a distinctive radial sand ridge topography, resulting in a segmented and striped distribution pattern of water depth (Figure 2a). The A–B section stations, located outside the radial sandbars and belonging to the Subei shoal, experience a relatively constant water depth of 15–20 m with minimal fluctuations between each station. Conversely, the C–F section stations fall within the range of the radial sandbars, exhibiting significant fluctuations in water depth. The G–I section stations show a clear increasing trend in water depth from the coast to the open sea.

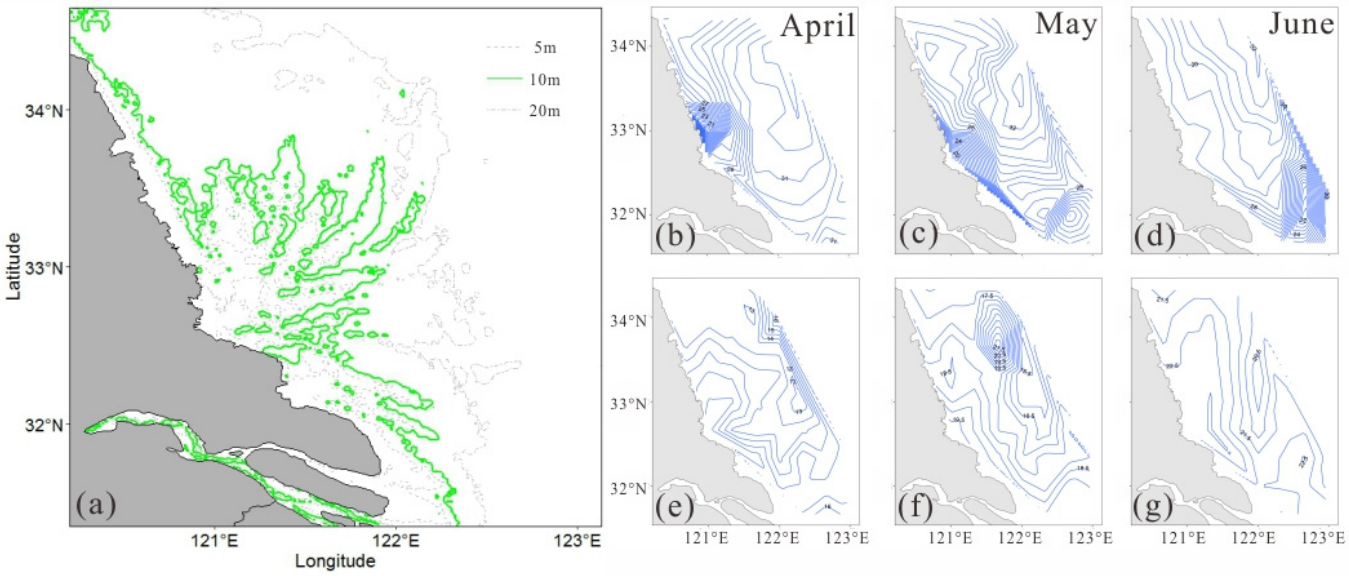

Figure 2. Characteristics of depth (**a**), temperature (**b**–**d**), and salinity (**e**–**g**) between April and June in the coastal waters of the southern Yellow Sea.

The monthly average temperature exhibits significant variation, with April experiencing the lowest average temperature at 14.3 °C and June having the highest average temperature at 21.9 °C (Figure 2b–d). The coastal waters of Jiangsu Province are influenced by both the land heat source and land monsoons, resulting in higher solar radiation and relatively higher seawater temperatures. As a result, the coastal waters of Jiangsu Province generally have slightly higher temperatures compared to those located further inland, with the southern part of the province having higher temperatures than the northern part. From April to May, the northeastern outer sea area is compressed by the cold water mass from the Yellow Sea, causing relatively dense isotherms and a large temperature gradient to form. Simultaneously, the coastal flow mixes with diluted water from the Yangtze River and transports it northward, contributing to the formation of a northward frontal structure near the coastline. In June, the dilution of water from the Yangtze River intensifies, leading to the expansion of the warm water front northward.

On the other hand, there is minimal variation in average salinity throughout the months, ranging from 28.9 to 29.7 (Figure 2e–g). Salinity gradually increases from nearshore areas to offshore areas. Near the coastal estuaries, a substantial amount of runoff water enters the ocean, resulting in a certain degree of seawater dilution and the formation of complex salinity gradient structures upon mixing with the ocean water. Specifically, in June, the influx of freshwater from the Yangtze River decreases the salinity levels in the surrounding areas of the Yangtze River estuary, forming a relatively low-salinity water mass and leading to significant changes in the isotherms.

3.2. Temporal and Spatial Distribution

A total of 3240 *L. polyactis* larvae, juveniles and young fish were collected. They were observed from April to June, with the peak occurring in May, reaching a density of 0.05 ind./m^3 (Figure 3). In the April samples, the distribution of developmental stages of fish was as follows: pre-flexion larvae (4%), flexion larvae (68%), post-flexion larvae (20%), and juveniles (7%). In the May samples, the distribution of developmental stages of fish was as follows: yolk-sac larvae (7%), pre-flexion larvae (70%), flexion larvae (3%), post-flexion larvae (1%), and juveniles (19%). In June, only 68 individuals were captured, and the dominant developmental stage was young (62%).

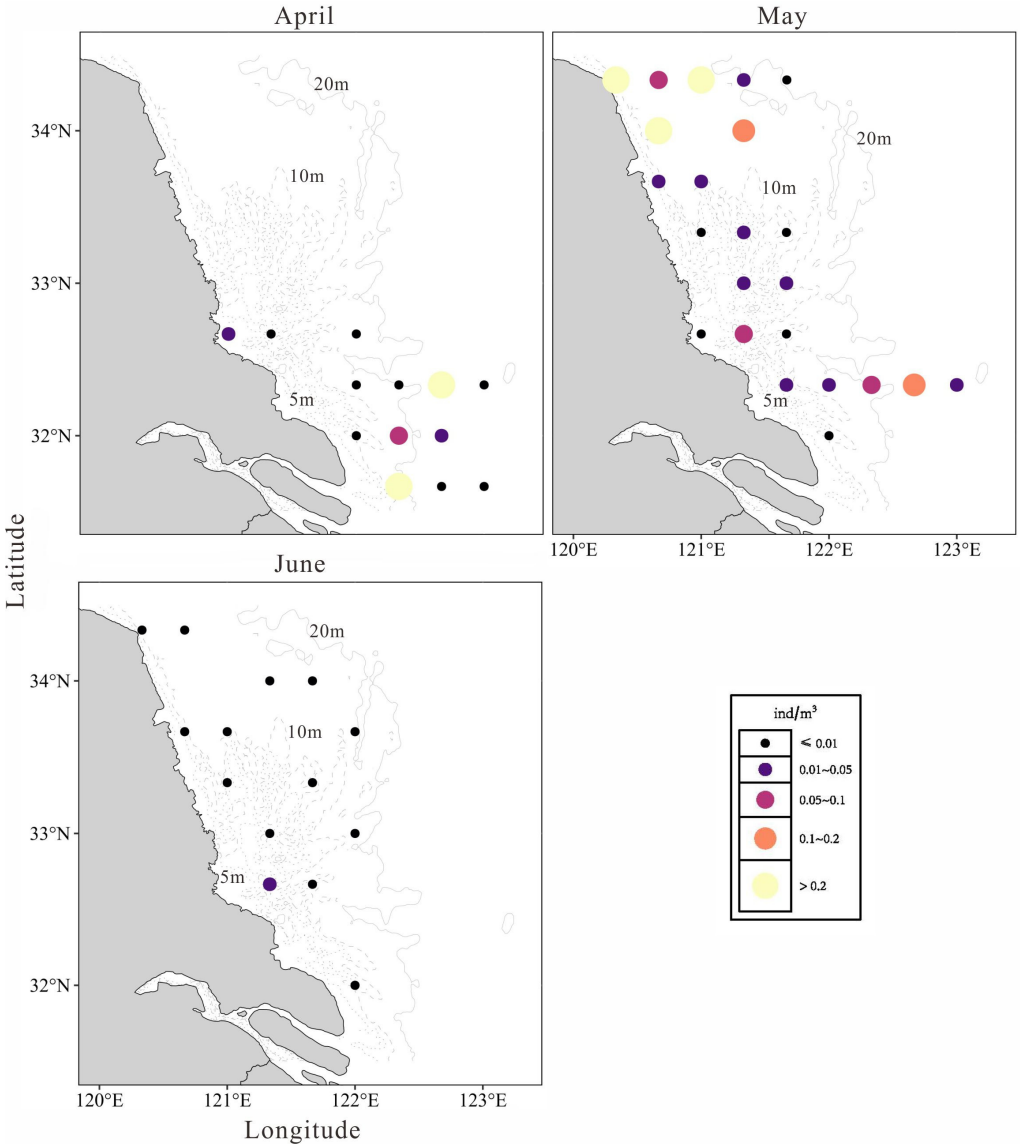

Figure 3. The density distribution of *L. polyactis* in early life stages from April to June.

The data reveal a clear signal that spawning occurs earlier in low-latitude areas (Figures 3 and 4). In April, *L. polyactis* only appear in the waters south of 32°40′ N, with a regulation that the later the development stage is, the closer its distribution is to the shore. The distribution range is the widest in May, with boundaries between 32° N and 34°20′ N. Nearshore stations exhibit higher density, gradually decreasing further offshore. The densely populated area is predominantly situated in the northern region, with the developmental stage progressively transitioning from early to late as one moves from north to south. In June, the occurrence rate is exceedingly low, and the density of occurrence at sampling stations is similarly minimal. The central nearshore waters serve as the distribution area for some of the earlier developmental stages, while the juvenile fish are distributed radially in the peripheral zones.

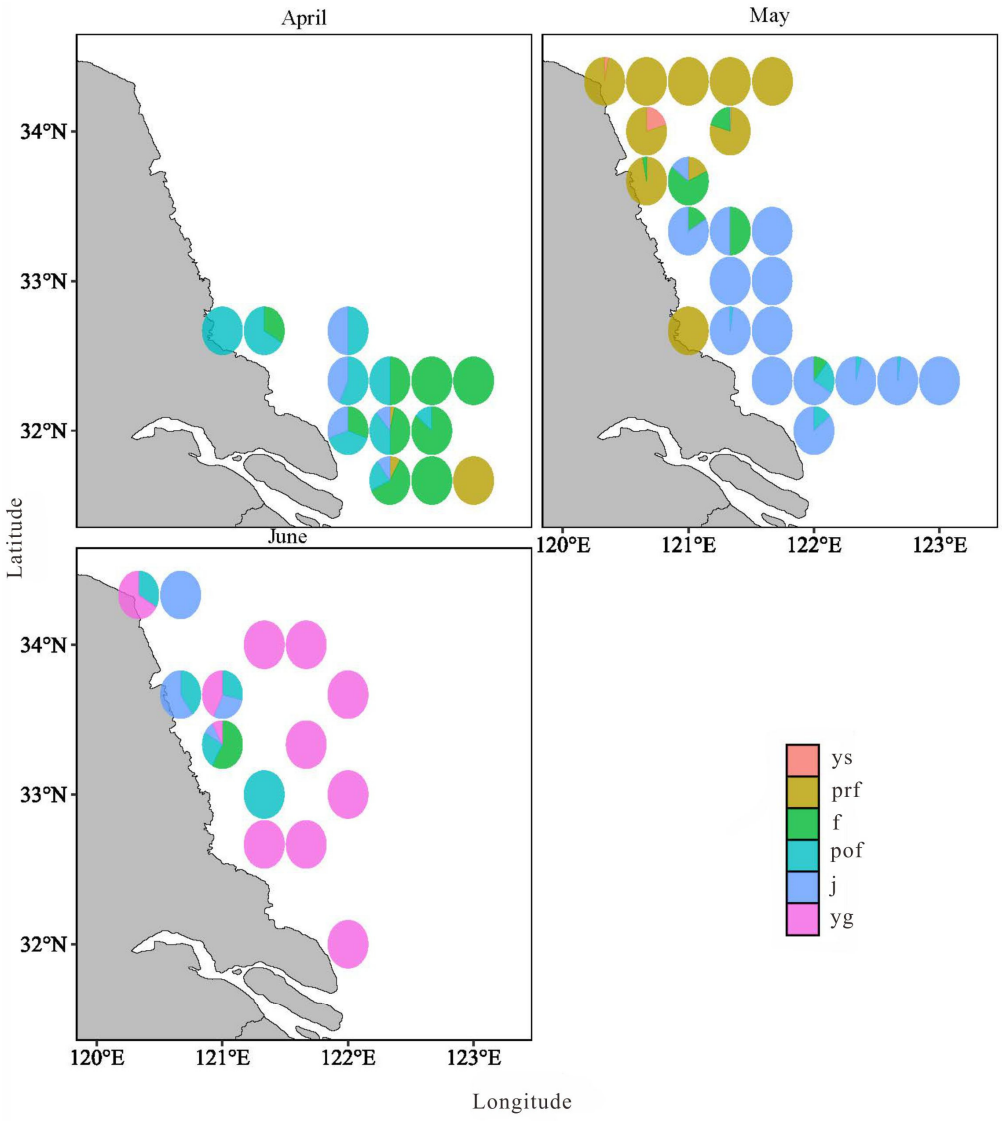

Figure 4. Distribution pattern at different developmental stages of *L. polyactis* (the size of the circle does not represent the density). ys = yolk-sac, prf = pre-flexion, f = flexion, pof = post-flexion, j = juvenile, yg = young.

3.3. Species Distribution Model

3.3.1. Model Evaluation

To identify deviations from the expected distribution, a QQ-plot was generated. The goodness of fit of the model to the data was assessed by comparing the consistency between expected residuals and observed residuals (Figure 5). DHARMa residual diagnostics

indicate a significant deviation for M3 and M4 in the Kolmogorov–Smirnov test (Table 2). The tests for models M1 and M2 are not significant, with M1 having the lowest AIC value (−76.8), suggesting it as the optimal model (Table 3).

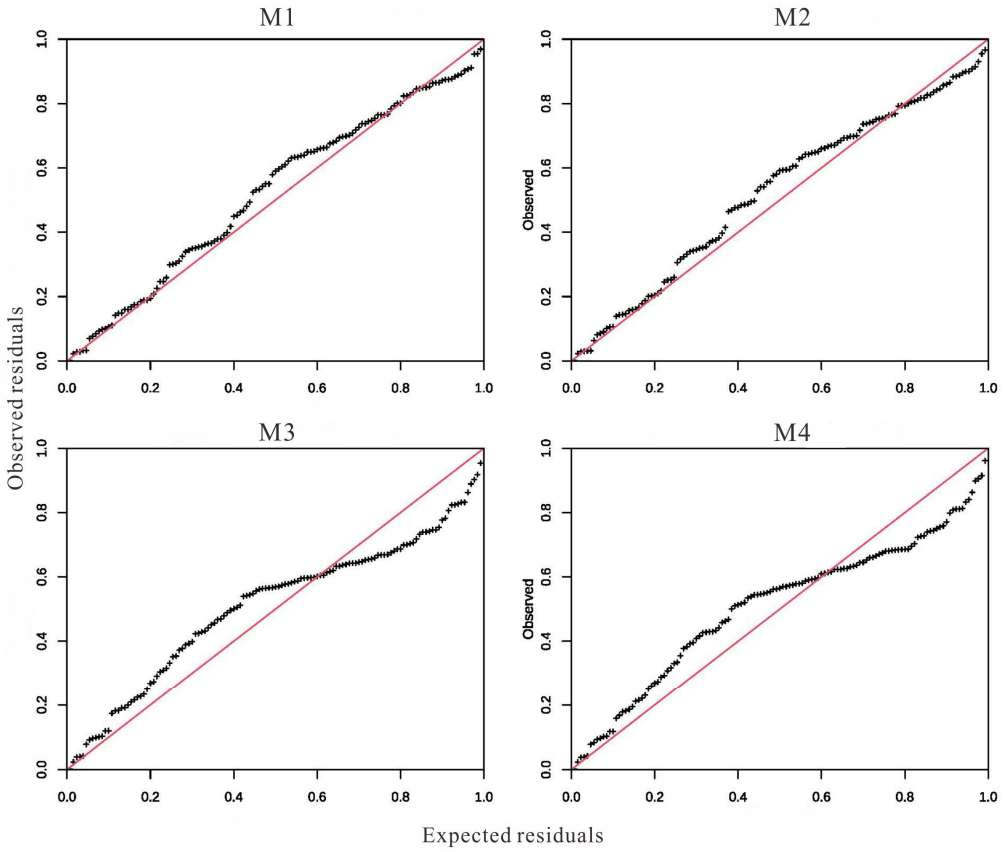

Figure 5. QQ-plot to detect overall deviations from the expected distribution. Residuals were calculated by the fitted models for the Tweedie distribution based on simulation and standardized to values between 0 and 1. *x*-axis shows expected value for uniform order statistics of residuals; *y*-axis shows observed residual value.

Table 2. Model adequacy diagnosis of models M1–M4 using Kolmogorov–Smirnov test.

Model	Statistics	*p* Value
M1	0.0946	0.1987
M2	0.0972	0.1743
M3	0.1531	0.0047
M4	0.1413	0.0116

Table 3. AIC model selection between models M1 and M2.

Model	AIC
M1	−76.8110
M2	−74.1120

3.3.2. The Relationship between *L. polyactis* Density and Environmental Factors

The scatter plot provides a visual depiction of the relationship between the density distribution of *L. polyactis* and the variables of depth, temperature, and salinity (Figure 6). Notably, the peak periods for the appearance of *L. polyactis* occur in April and May, with a consistent distribution depth between 14 and 30 m. However, in June, the density distribution shifts towards shallower coastal waters, with a higher concentration in areas

shallower than 15 m. The temperature range suitable for the survival of *L. polyactis* is extensive, with a noticeable increase from April to June, indicating the environmental plasticity of the reproductive strategy of *L. polyactis*. The salinity of *L. polyactis* aggregation areas remains relatively stable, ranging primarily between 28 and 30‰ throughout the months, with minimal occurrence of *L. polyactis* in low-salinity waters.

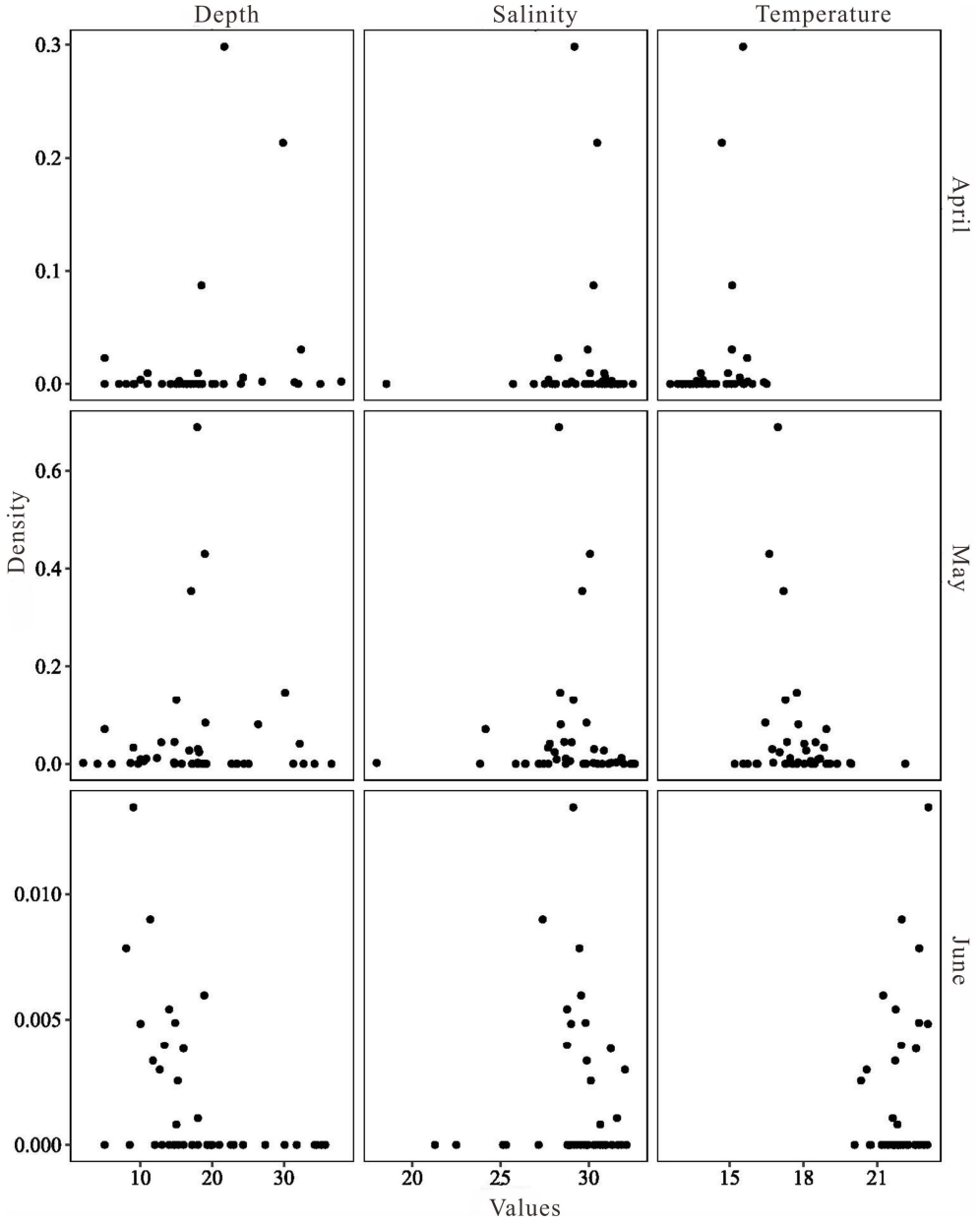

Figure 6. Scatter plot of relationship between density of *L. polyactis* and environmental factors.

The M1 model predicts that the monthly variation in *L. polyactis* density depends on temperature, providing a more refined understanding of the temperature-dependent variation (Figure 7). In April, the density of *L. polyactis* gradually increases within the temperature range of 12.5–16.5 °C. In May, *L. polyactis* reach their peak density at 16.5–17.5 °C, after which further temperature increase does not promote an increase in *L. polyactis* density; instead, it shows a decreasing trend. June is predicted to have the highest *L. polyactis* density, but observations show that *L. polyactis* only appear at temperatures above 20 °C, with lower density values than those in April and May.

Furthermore, salinity exhibits a nonlinear effect on *L. polyactis* density, with occurrences rare at low salinities (Figure 8). When salinity exceeds 27.5‰, *L. polyactis* start to appear

in large numbers, reaching the maximum value at 29‰. Above 30‰, *L. polyactis* density gradually decreases. This impact of salinity on *L. polyactis* density is consistent across months, indicating salinity as a stable indicator influencing the density of *L. polyactis*.

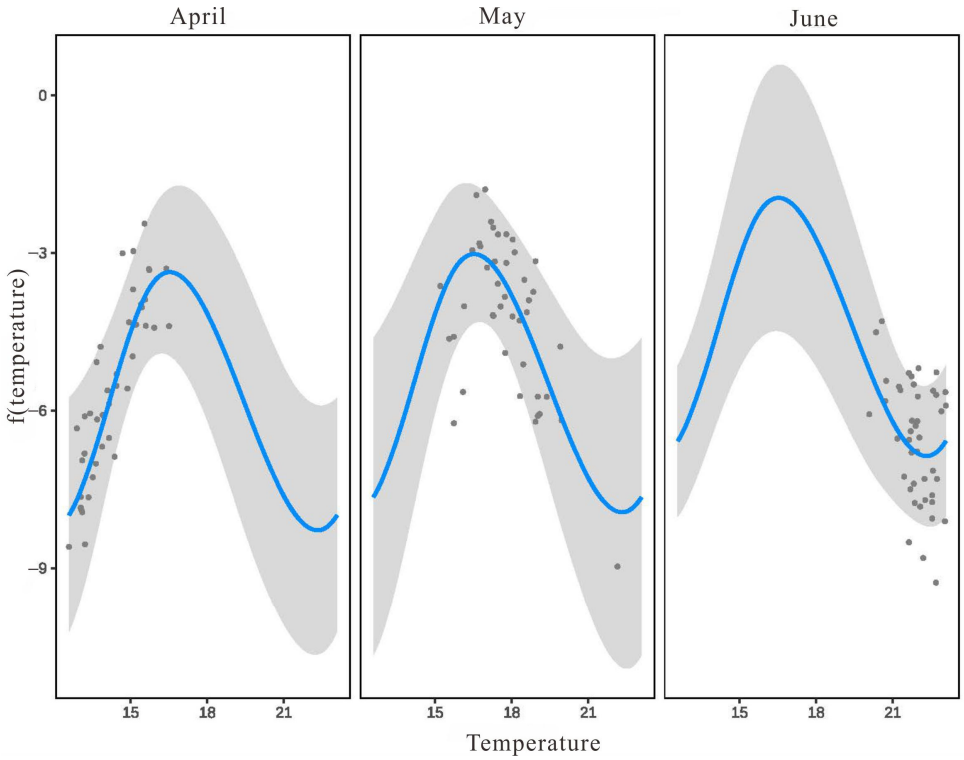

Figure 7. Effect of temperature on the density of *L. polyactis* using sdmTMB. The grey shade area represents the 95% confidence interval.

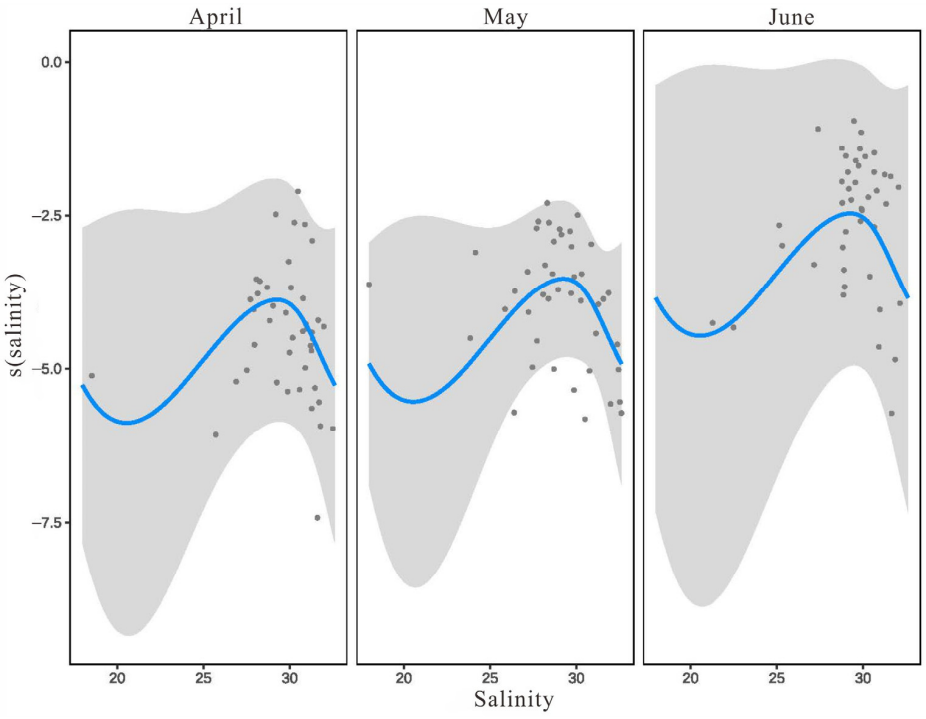

Figure 8. Effect of salinity on the density of *L. polyactis* using sdmTMB. The grey shade area represents the 95% confidence interval.

3.3.3. Model Prediction

The predicted values of *L. polyactis* density show high spatial consistency with the observed values (Figure 9), indicating a spatial distribution pattern of *L. polyactis* that varies between months. In April, the surface water temperature in the southern region is generally higher than that in the northern region, and the range of *L. polyactis* aggregation is very small, concentrated only in the higher-temperature areas of the Yangtze River estuary and the offshore waters of Lvsi. In May, as the temperature rises, *L. polyactis* are widely distributed in the coastal waters of Jiangsu, with the most concentrated area appearing in the waters north of 34° N and spreading south along the coastline. Additionally, the section at 32.5° N also shows higher *L. polyactis* fish density. In June, *L. polyactis* density significantly decreases, mainly occurring in the waters north of 32.5° N, with a narrow and elongated distribution along the coastline.

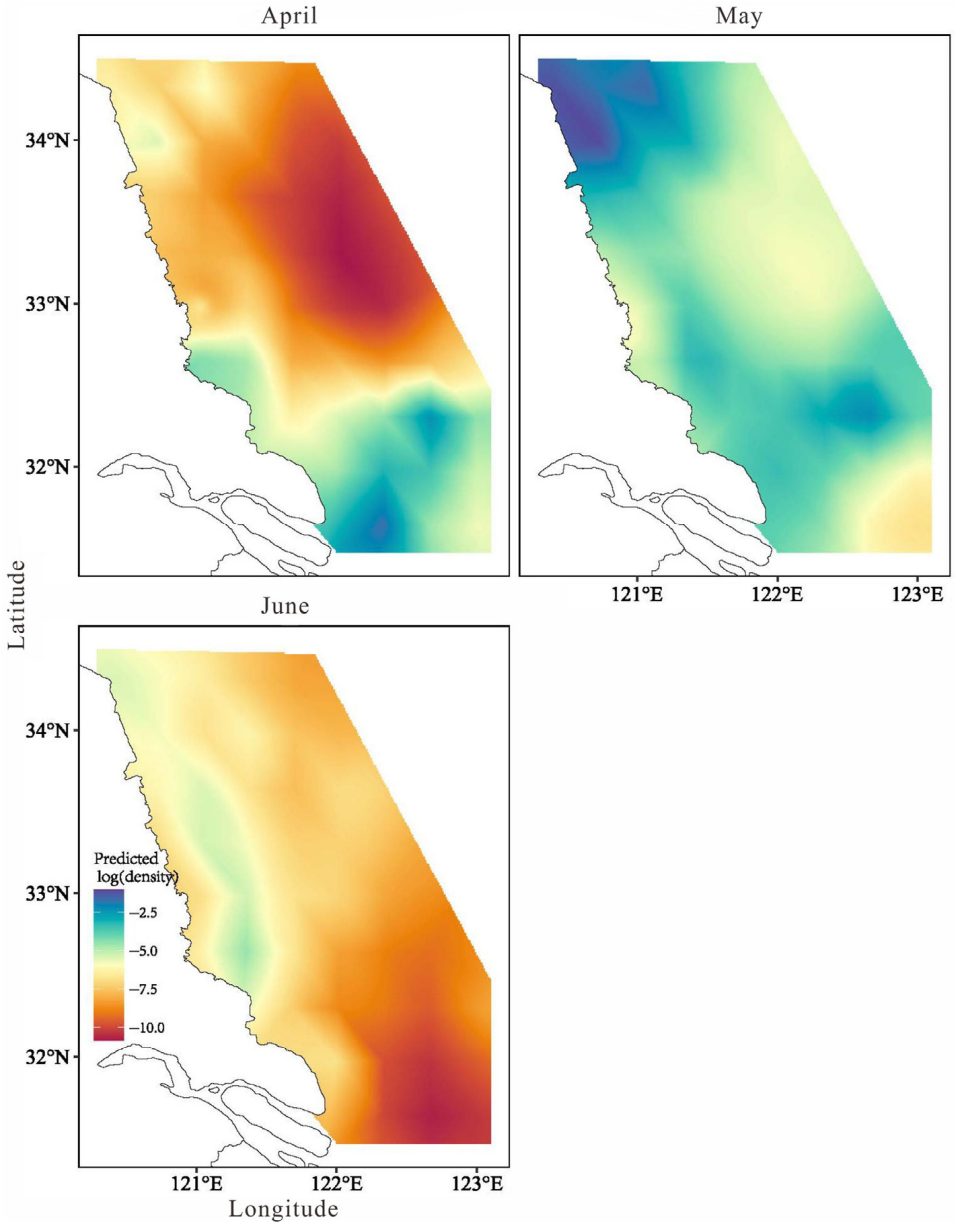

Figure 9. The predicted density distribution of *L. polyactis* using sdmTMB from the year 2019.

4. Discussion

Coastal gradients play a vital role in shaping the distribution patterns of early life stages of fish, as highlighted by the findings of this study on *L. polyactis*. The concentration

of pre-flexion larval fish in the waters north of 33°30′ N in May represents a link between the distribution patterns and the parental selection of spawning grounds. Yin et al. identified that the region is located at the periphery of the Yellow Sea Cold Water Mass, being concurrently affected by a suite of physical processes such as coastal dilution water, the Lu'nan Coastal Current, and the Subei Coastal Current [22]. These processes collectively contribute to the formation of temperature and salinity gradients, which in turn stimulate the development of the *L. polyactis* gonads, creating a spawning ground for this species. Our research indicates that the distribution area of pre-flexion larvae of *L. polyactis* is near the spawning ground. This is primarily because the eggs need up to approximately ten days to develop into pre-flexion larvae [21]. Due to their limited swimming capabilities at this stage, pre-flexion larvae predominantly depend on water currents for drift. Considering that the Yellow Sea Coastal Current in this region flows at a speed of only 0.1–0.2 m/s [43], and the area is positioned in a buffer zone between the tidal waves of the southwestern Yellow Sea and the counterpropagating tidal waves of the northern Yellow Sea [44], this constrains the long-distance dispersal of the larvae. Specifically, the Yangtze River and the multiple Subei local rivers (SLRs) contribute to the formation of low-salinity coastal water in 33.5–34.5° N, which are greatly controlled by the tidal residual currents. The unique tide system in the southwestern Yellow Sea generates a northward residual current south of 33.5° N and a southward residual current north of 34.5° N, which converge and propagate offshore in the vicinity of the Old Yellow River Delta [25,45]. Accumulation of larvae due to thermoclines and haloclines in stratified water bodies (stable ocean hypothesis) results in spatial and temporal overlap with suitable planktonic prey [46,47], which can attract and support their growth and survival [26].

Bathymetry, or the underwater topography, is another coastal feature that can influence early fish distribution. Variation in bathymetry along the coastline can create different habitats and physical conditions for larvae and juvenile fish. In the South Yellow Sea, the tidal wave system and the fluvial sediment supply shaped the largest RSRs; one of the typical characteristics of the RSRs is their asymmetric pattern, showing smaller southern sand ridges than the northern ones [48]. This asymmetry is attributed to rotary currents with increasing ellipticity, which are induced by progressive waves propagating from the East China Sea [49]. In April, flexion larvae and post-flexion larvae of *L. polyactis* concentrated in the southern radiating sand ridges. Xiong et al. suggested that eddies retained larvae within the natal area and influenced their ability to recruit to the juvenile habitat [50]. In May, juveniles surpassing 30 days of age exhibit robust swimming capabilities, possess the autonomy to select their aquatic habitat, and are widely dispersed across both the northern and southern sand ridges. Similarly, through the otolith Sr/Ca value change, Xiong et al. revealed that individuals less than 37–41 days old during the pelagic phase swam in the inertial hydrodynamic regime of residual eddies in the sandy ridge system [50]. Moreover, RSR regions are characterized by higher nutrient concentrations due to the terrestrial runoff [51,52]. These nutrient inputs can enhance primary productivity, leading to increased food availability for pelagic-phase fish [52–54].

The distinct spatial variations in early life fish abundance at different developmental stages indicate the utilization of different habitats for nursery purposes. Pre-flexion and post-flexion larvae prior to metamorphosis showed high distribution heterogeneity (Figure 4). Studies on the early life history of various marine fish have also shown that larval fish exhibit specific habitat preferences based on their developmental stage [55]. This suggests that the utilization of different habitats for spawning and nursery purposes is a common phenomenon among marine fish species. In fish ecology, habitat requirements are generally assigned to ontogenetic levels rather than to development stages on a specific ontogenetic level [56–58]. However, our results demonstrate that ontogenetic shifts in habitat use also exist in early life history stages, including nearshore and inshore habitats of the system. In the south of Jiangsu, *L. polyactis* spawn in nearshore waters; after hatching, larvae in the pre-flexion stage remained aggregated in the vicinity of the spawning beds [22]. However, larvae in the advanced development stage (post-flexion)

and juveniles left the nearshore and moved towards inshore habitats of the coast (Figure 4); one reason for this behavior is the presence of multiple rivers, such as the Huai River and Sheyang River, which flow into the sea in this area and provide abundant food sources. In contrast, in the north of Jiangsu, fish in the pre-flexion stages were abundant in the inshore and nearshore habitats, and juveniles were found to be increasingly dispersed throughout the nearshore water of the coast (Figure 4). Generally, larval and juvenile fish movement towards nursery ground habitats by either passive or active dispersal mechanisms has been widely described for ocean spawning fish [59,60]. Xiong et al. analyzed the variations of otolith elements in juvenile *L. polyactis*, suggesting that the juveniles disperse between early April and early May, inhabit sandy ridges to feed, and migrate offshore in late June, which is consistent with our findings [50].

The timing of reproduction in fish species is a critical aspect of their life history strategy and can be influenced by various environmental factors. The earlier spawning in low-latitude areas suggests that the reproductive timing of *L. polyactis* is influenced by temperature [26]. The spawning grounds of *L. polyactis* in the East China Sea zone encompass a broad latitudinal range of 26°30′ N to 35°00′ N. *L. polyactis* start to spawn in Jiangsu waters in April, with temperature ranges between 13 °C and 16 °C. However, we have identified post-flexion larvae and juveniles in the waters of Jiangsu, which may originate from the small yellow croaker spawning grounds in northern Zhejiang. The analysis of oceanographic conditions by Xu et al. provides additional evidence in support of this hypothesis [13]. The peak spawning period occurs in May, aligning with ideal habitat temperatures ranging from 16.5 °C to 18.5 °C. The spawning activities gradually move northward as the temperature rises in the northern region. Pankhurst and Munday indicated that increasing temperatures cue reproductive development in spring-spawning species [61]. Similarly, Asch et al. indicated that shifts in oceanography and temperature have led to changes in the timing of reproductive events in the California Current [62]. The mechanism underlying the influence of temperature on reproductive timing may be linked to its impact on the endocrine system and gonadal development of the fish. The reproductive cycle in fish is under the control of the brain–pituitary–gonad (BPG) axis. External environmental stimuli trigger the release of gonadotropin-releasing hormone (GnRH) from the hypothalamus of the brain, which regulates the recreation of gonadotropin (follicle-stimulating hormone, FSH, and luteinizing hormone, LH) from the pituitary gland. FSH regulates the gonad development and LH regulates the final maturation and spawning [63].

Phenological character such as peak spawning time may vary within and differ between populations in relation to environmental factors [64]. *Larimichthys polyactis* exhibits regional variations in reproductive timing, suggesting a diverse response to temperature across different areas. The plasticity of reproductive temperature refers to the ability of fishes to adjust their reproductive timing in response to variations in temperature. Fish species with a wider range of temperature tolerance are better equipped to cope with changing environmental conditions, which allows fish populations to optimize their reproductive success. Salmon can adjust their spawning time in response to temperature variations, ensuring that their larvae are released during favorable thermal conditions [65,66]. Fish populations with higher temperature adaptability had a greater capacity to persist and recover from disturbances caused by temperature fluctuations [67–70]. The ecological adaptability of *L. polyactis* in response to temperature variations has broader implications for its distribution and abundance in different habitats. The species' ability to adjust its reproductive timing in accordance with local temperature regimes enables it to exploit a wide range of environmental conditions, contributing to its ecological success in diverse marine ecosystems [71]. The sister species of *L. polyactis*, known as *L. crocea*, has been subjected to fishing activities for a similar duration as its smaller counterpart. However, *L. crocea* exhibits a narrower range of temperature adaptation and experienced a decline in population during the late 1970s [72]. While excessive fishing was identified as the primary cause of *L. crocea* collapse, Wang et al. concluded that climate-induced changes in overwintering habitat suitability may have exacerbated the fishery collapse of the *L. crocea*

population [73]. This thermal adaptation is often an important reason for whether invasive species or reintroduced species are able to settle down and expand their populations in the field of invasion ecology [74].

The identification and conservation of nursery habitats are pivotal for the sustainable management of fish populations [75]. The presence of mainly juveniles in the southern waters below 33° N suggests the utilization of these areas as nursery habitats for *L. polyactis*. Understanding the importance of these nursery grounds can help inform conservation efforts and ensure the recruitment and survival of juvenile fish [76]. Many fish species exhibit ontogenetic shifts in habitat use, with larvae and juveniles utilizing different habitats for nursery purposes [77,78]. This strategy allows for the increased survival and growth of larvae, as nursery habitats often provide more favorable conditions and resources compared to other areas. Targeted conservation measures can be implemented to protect and enhance these nursery habitats. For example, the establishment of marine protected areas (MPAs) can help protect critical nursery habitats from destructive fishing practices and habitat degradation [79]. MPAs can also contribute to the restoration and enhancement of degraded habitats, which can benefit the recruitment and survival of larvae and juvenile fish. Fortunately, a germplasm resource reserve for *L. polyactis* has been established at 32°12′–34°00′ N, effectively safeguarding the breeding population and offspring of this species. Furthermore, the area north of the Yangtze River estuary to 32°10′ N has been designated as an ecological red line, prohibiting any development or utilization activities, thereby creating a comprehensive spawning population and reserve for larvae and juvenile *L. polyactis*. In the northern Jiangsu sea Haizhou Bay, habitat restoration efforts, such as the creation of artificial reefs or the improvement of water quality, enhanced the availability and quality of nursery habitats for the larval *L. polyactis* [80,81]. However, there are some limitations for improvement in conserving *L. polyactis* nursery habitats. Firstly, identifying and characterizing nursery habitats can be challenging due to the dynamic nature of coastal ecosystems and the complex interactions between fish and their environment. For instance, the continuous horizontal tow method may not fully capture the diel vertical migration behavior exhibited by larvae fish, particularly during their post-larval stages and juveniles [82,83]. This migratory pattern could lead to significant fluctuations in fish abundance at the surface throughout the day, potentially biasing data representation of their spatial and temporal distribution. Further research is needed to better understand the specific habitat preferences and diel vertical migration behavior of *L. polyactis* during their early life stages. Second, the Yangtze River Estuary serves as a crucial nursery ground for *L. polyactis*, a species vulnerable to the dual impacts of climate change and human activities within the Yangtze River basin. Fluctuations in the Yangtze's freshwater flow alter the salinity conditions of the area, potentially leading to increased suspended sediment and eutrophication of the water, which in turn affect the growth of algae and the early survival rate of *L. polyactis* [84,85]. Moreover, the spawning grounds in southern Jiangsu and northern Zhejiang are interconnected with the nursery grounds at the Yangtze River Estuary, underscoring the need for comprehensive conservation planning that considers the environmental conditions of different regions and establishes a network of protected areas. Finally, despite the establishment of *L. polyactis* germplasm resource reserves as early as 2009, there has been a lack of systematic evaluation of the management effectiveness. The absence of such assessments makes it difficult to accurately understand the actual impact of conservation measures and to adjust and optimize strategies accordingly. Therefore, enhancing the evaluation of the management effectiveness of *L. polyactis* germplasm resource reserves is of significant importance for improving the scientific and effective nature of conservation efforts.

5. Conclusions

Through field investigation and comprehensive analysis, we revealed the ecological habits of *L. polyactis* larvae and juveniles in the nursery ground of the southern Yellow Sea, including their distribution range, migration path and dispersal characteristics. There was

a broad temperature tolerance for *L. polyactis* survival and the distribution areas varied from April to June. After hatching, the pre-flexion larvae tend to remain aggregated near the spawning beds; the post-flexion larvae and juveniles move towards the sandy ridge habitats along the coast and start to migrate offshore in June. This study provides valuable insights for the effective management of fishery resources in the area and can be utilized to identify marine areas with specific habitat features that require conservation.

Author Contributions: Investigation, X.S., M.X., Y.Z. and J.L.; formal analysis, X.S.; writing—original draft, X.S.; resources, F.H. and J.C.; data curation, F.H.; methodology, Y.J. and X.G.; software, Z.L. and S.L.; writing—review and editing, Z.L.; project administration, S.L. and J.C. All authors have read and agreed to the published version of the manuscript.

Funding: This work was supported by the Central Public-Interest Scientific Institution Basal Research Fund, East China Sea Fisheries Research Institute, Chinese Academy of Fishery Sciences (2019M05); the Basic Research Fund for State-Level Nonprofit Research Institutes of ESCFRI, CAFS (#Dong2022TD01); and the Special Funds for Survey of Nearshore Spawning Ground by the Ministry of Agriculture and Rural Affairs, China (125C0505).

Institutional Review Board Statement: Not applicable.

Informed Consent Statement: Not applicable.

Data Availability Statement: Data will be available on reasonable request from the corresponding author.

Conflicts of Interest: The authors declare no conflicts of interest.

References

1. Takatsu, T.; Toyonaga, T.; Hirao, S.; Ooka, E.; Kobayashi, N.; Nakaya, M. Spawning ground selection and larval feeding habits of Arabesque greenling *Pleurogrammus azonus* around the Matsumae Peninsula, Japan. *Fish. Sci.* **2024**, *90*, 435–452. [CrossRef]
2. Arevalo, E.; Cabral, H.N.; Villeneuve, B.; Possémé, C.; Lepage, M. Fish larvae dynamics in temperate estuaries: A review on processes, patterns and factors that determine recruitment. *Fish Fish.* **2023**, *24*, 466–487. [CrossRef]
3. Tyler, K.J.; Wedd, D.; Crook, D.; Kennard, M.; King, A.J. Hydrology drives variation in spawning phenologies and diversity of larval assemblages of Australian wet–dry tropical fish. *Freshw. Biol.* **2021**, *66*, 1949–1967. [CrossRef]
4. Brosset, P.; Smith, A.D.; Plourde, S.; Castonguay, M.; Lehoux, C.; Van Beveren, E. A fine-scale multi-step approach to understand fish recruitment variability. *Sci. Rep.* **2020**, *10*, 16064. [CrossRef]
5. Liu, Z.L.; Jin, Y.; Yang, L.L.; Yuan, X.W.; Yan, L.P.; Zhang, Y.; Zhang, H.; Xu, M.; Song, X.J.; Tang, J.H.; et al. Improving prediction for potential spawning areas from a two-step perspective: A comparison of multi-model approaches for sparse egg distribution. *J. Sea Res.* **2023**, *197*, 102460. [CrossRef]
6. Guerreiro, M.A.; Martinho, F.; Baptista, J.; Costa, F.; Pardal, M.A.; Primo, A.L. Function of estuaries and coastal areas as nursery grounds for marine fish early life stages. *Mar. Environ. Res.* **2021**, *170*, 105408. [CrossRef] [PubMed]
7. Acha, E.M.; Piola, A.; Iribarne, O.; Mianzan, H. Biology of Fronts. In *Ecological Processes at Marine Fronts*; Springer: Cham, Switzerland, 2015.
8. Zheng, J.; Gao, T.X.; Yan, Y.R.; Song, N. Genetic variation of the small yellow croaker (*Larimichthys polyactis*) inferred from mitochondrial DNA provides novel insight into the fluctuation of resources. *Acta Oceanol. Sin.* **2022**, *41*, 88–95. [CrossRef]
9. Lin, L.S.; Liu, Z.L.; Jiang, Y.Z.; Huang, W.; Gao, T.X. Current status of small yellow croaker resources in the southern Yellow Sea and the East China Sea. *Chin. J. Oceanol. Limnol.* **2011**, *29*, 547–555. [CrossRef]
10. Zhang, C.; Ye, Z.J.; Wan, R.; Ma, Q.Y.; Li, Z.G. Investigating the population structure of small yellow croaker (*Larimichthys polyactis*) using internal and external features of otoliths. *Fish. Res.* **2014**, *153*, 41–47. [CrossRef]
11. Li, Z.L.; Shan, X.J.; Jin, X.S.; Dai, F.Q. Long-term variations in body length and age at maturity of the small yellow croaker (*Larimichthys polyactis* Bleeker, 1877) in the Bohai Sea and the Yellow Sea, China. *Fish. Res.* **2011**, *110*, 67–74. [CrossRef]
12. Liang, Z.L.; Sun, P.; Yan, W.; Huang, L.Y.; Tang, Y.L. Significant effects of fishing gear selectivity on fish life history. *J. Ocean Univ. China* **2014**, *13*, 467–471. [CrossRef]
13. Xu, M.; Wang, Y.H.; Liu, Z.L.; Liu, Y.; Zhang, Y.; Yang, L.L.; Wang, F.; Wu, H.; Cheng, J.H. Seasonal distribution of the early life stages of the small yellow croaker (*Larimichthys polyactis*) and its dynamic controls adjacent to the Changjiang River Estuary. *Fish. Oceanogr.* **2023**, *32*, 390–404. [CrossRef]
14. Koenigbauer, S.T.; Höök, T.O. Increased offspring provisioning by large female fish and consequences for reproductive efficiency. *Ecol. Evol.* **2023**, *13*, e10555. [CrossRef]
15. Grüss, A.; Biggs, C.; Heyman, W.D.; Erisman, B. Prioritizing monitoring and conservation efforts for fish spawning aggregations in the US Gulf of Mexico. *Sci. Rep.* **2018**, *8*, 8473.

16. Dambrine, C.; Woillez, M.; Huret, M.; de Pontual, H. Characterising Essential Fish Habitat using spatio-temporal analysis of fishery data: A case study of the European seabass spawning areas. *Fish. Oceanogr.* **2021**, *30*, 413–428. [CrossRef]
17. Laman, E.A.; Rooper, C.N.; Turner, K.; Rooney, S.; Cooper, D.W.; Zimmermann, M. Using species distribution models to describe essential fish habitat in Alaska. *Can. J. Fish. Aquat. Sci.* **2018**, *75*, 1230–1255. [CrossRef]
18. Zhong, X.M.; Zhang, H.; Tang, J.H.; Zhong, F.; Zhong, J.S.; Xiong, Y.; Gao, Y.S.; Ge, K.K.; Yu, W.W. Temporal and spatial distribution of *Larimichthys polyactis* Bleeker resources in offshore areas of Jiangsu Province. *J. Fish. China* **2011**, *235*, 238–246.
19. Lin, N.; Chen, Y.G.; Jin, Y.; Yuan, X.W.; Ling, J.Z.; Jiang, Y.Z. Distribution of the early life stages of small yellow croaker in the Yangtze River estuary and adjacent waters. *Fish. Sci.* **2018**, *84*, 357–363. [CrossRef]
20. Wang, Y.L.; Hu, C.L.; Xu, K.D.; Zhou, Y.D.; Jiang, R.J.; Li, Z.H.; Li, X.F. Reproductive Status of *Larimichthys polyactis* in Zhoushan Fishing Ground and Adjacent Waters from 2020 to 2021. *Ocean Dev. Manag.* **2022**, *39*, 53–57.
21. Zhan, W.; Lou, B.; Chen, R.Y.; Mao, G.M.; Liu, F.; Xu, D.D.; Wang, L.G.; Ma, T.; Xu, Q.X. Observation of embryonic, larva and juvenile development of small yellow croaker, *Larimichthys polyactis*. *Oceanol. Limnol. Sin.* **2016**, *47*, 1033–1039.
22. Yin, J.; Wang, J.; Zhang, C.L.; Xu, B.D.; Xue, Y.; Ren, Y.P. Spatial and temporal distribution characteristics of *Larimichthys polyactis* eggs in Haizhou Bay and adjacent regions based on two-stage GAM. *J. Fish. Sci. China* **2019**, *26*, 1164–1174.
23. Nakazawa, T. Ontogenetic niche shifts matter in community ecology: A review and future perspectives. *Popul. Ecol.* **2015**, *57*, 347–354. [CrossRef]
24. Rao, W.B.; Mao, C.P.; Wang, Y.G.; Su, J.B.; Balsam, W.; Ji, J.F. Geochemical constraints on the provenance of surface sediments of radial sand ridges off the Jiangsu coastal zone, East China. *Mar. Geol.* **2015**, *359*, 35–49. [CrossRef]
25. Zhou, F.; Su, J.L.; Huang, D.J. Study on the intrusion of coastal low salinity water in the west of southern Huanghai Sea during spring and summer. *Haiyang Xuebao* **2004**, *26*, 34–44.
26. Liu, Z.L.; Jin, Y.; Yang, L.L.; Yan, L.P.; Zhang, Y.; Xu, M.; Tang, J.H.; Zhou, Y.D.; Hu, F.; Cheng, J.H. Incorporating egg-transporting pathways into conservation plans of spawning areas: An example of small yellow croaker (*Larimichthys polyactis*) in the East China Sea zone. *Front. Mar. Sci.* **2022**, *9*, 941411. [CrossRef]
27. Ahlstrom, E.H.; Moser, H.G. Eggs and larvae of fishes and their role in systematic investigations and in fisheries. *Rev. Trav. L'institut Peches Marit.* **1976**, *40*, 379–398.
28. Ahlstrom, E.H.; Moser, H.G. Systematics and development of early life history stages of marine fishes: Achievements during the past century, present status and suggestions for the future. *Rapp. P.-V. Réun. Cons. Int. Explor. Mer.* **1981**, *178*, 541–546.
29. Miller, B.S.; Kendall, A.W.J. *Early Life History of Marine Fishes*; University of California Press: London, UK, 2009.
30. Zhang, R.Z.; Lu, H.F.; Zhao, C.Y.; Chen, L.F.; Zang, Z.J.; Jiang, W.Y. *Fish Eggs and Larvae in the Offshore Waters of China*; Shanghai Scientific & Technical Publishers: Shanghai, China, 1985.
31. Anderson, S.C.; Ward, E.J.; English, P.A.; Barnett, L.A.K. sdmTMB: An R package for fast, flexible, and user-friendly generalized linear mixed effects models with spatial and spatiotemporal random fields. *bioRxiv* **2022**, 485545. [CrossRef]
32. Lindgren, F.; Rue, H. Bayesian Spatial Modelling with R-INLA. *J. Stat. Softw.* **2015**, *63*, 1–25. [CrossRef]
33. Kristensen, K.; Nielsen, A.; Berg, C.W.; Skaug, H.; Bell, B.M. TMB: Automatic Differentiation and Laplace Approximation. *J. Stat. Softw.* **2016**, *70*, 1–21. [CrossRef]
34. Commander, C.J.C.; Barnett, L.A.K.; Ward, E.J.; Anderson, S.C.; Essington, T.E. The Shadow Model: How and Why Small Choices in Spatially Explicit Species Distribution Models Affect Predictions. *Peerj* **2022**, *10*, e12783. [CrossRef]
35. Grüss, A.; Drexler, M.; Ainsworth, C.H. Using Delta Generalized Additive Models to Produce Distribution Maps for Spatially Explicit Ecosystem Models. *Fish. Res.* **2014**, *159*, 11–24. [CrossRef]
36. Thorson, J.T.; Cunningham, C.J.; Jorgensen, E.; Havron, A.; Hulson, P.J.F.; Monnahan, C.C.; von Szalay, P. The surprising sensitivity of index scale to delta-model assumptions: Recommendations for model-based index standardization. *Fish. Res.* **2021**, *233*, 105–745. [CrossRef]
37. Thorson, J.T.; Shelton, A.O.; Ward, E.J.; Skaug, H.J. Geostatistical Delta-Generalized Linear Mixed Models Improve Precision for Estimated Abundance Indices for West Coast Groundfishes. *Ices J. Mar. Sci.* **2015**, *72*, 1297–1310. [CrossRef]
38. Post, S.; Fock, H.O.; Jansen, T. Blue whiting distribution and migration in Greenland waters. *Fish. Res.* **2019**, *212*, 123–135. [CrossRef]
39. Barnett, L.A.K.; Ward, E.J.; Anderson, S.C. Improving estimates of species distribution change by incorporating local trends. *Ecography* **2020**, *44*, 427–439. [CrossRef]
40. Evans, A.L.; Bulla, A.J.; Kieta, A.R. The precision teaching system: A synthesized definition, concept analysis, and process. *Behav. Anal. Pract.* **2021**, *14*, 559–576. [CrossRef] [PubMed]
41. Li, C.X.; Deroba, J.J.; Miller, T.J.; Legault, C.M.; Perretti, C.T. An evaluation of common stock assessment diagnostic tools for choosing among state-space models with multiple random effects processes. *Fish. Res.* **2024**, *273*, 106968. [CrossRef]
42. Hartig, F. DHARMa: Residual Diagnostics for Hierarchical (Multi-Level/Mixed) Regression Models. R package version 0.4.6. 2022. Available online: https://cran.r-project.org/web/packages/DHARMa/vignettes/DHARMa.html (accessed on 6 April 2023).
43. Chen, M.Y.; Zeng, C.; Zeng, X.; Liu, Y.; Wang, Z.H.; Shi, X.J.; Cao, L. Assessment of marine protected areas in the East China Sea using a management effectiveness tracking tool. *Front. Mar. Sci.* **2023**, *10*, 1081036. [CrossRef]
44. Wu, H.; Gu, J.H.; Zhu, P. Winter Counter-Wind Transport in the Inner Southwestern Yellow Sea. *J. Geophys. Res.-Ocean.* **2018**, *123*, 411–436. [CrossRef]

45. Zhu, P.; Wu, H. Origins and transports of the low-salinity coastal water in the southwestern Yellow Sea. *Acta Oceanol. Sin.* **2018**, *37*, 1–11. [CrossRef]
46. Lasker, R. The relation between oceanographic conditions and larval anchovy food in the California Current: Identification of factors contributing to recruitment failure. *Rapp. P.-V. Réun. Cons. Int. Explor. Mer.* **1978**, *173*, 212–230.
47. Cushing, D. Plankton production and year-class strength in fish populations: An update of the match/mismatch hypothesis. *Adv. Mar. Biol.* **1990**, *26*, 249–293.
48. Tao, J.F.; Wang, Z.B.; Zhou, Z.; Xu, F.; Zhang, C.K.; Stive, M.J.F. A Morphodynamic Modeling Study on the Formation of the Large-Scale Radial Sand Ridges in the Southern Yellow Sea. *J. Geophys. Res.-Earth* **2019**, *124*, 1742–1761. [CrossRef]
49. Xu, F.; Tao, J.F.; Zhou, Z.; Coco, G.; Zhang, C.K. Mechanisms underlying the regional morphological differences between the northern and southern radial sand ridges along the Jiangsu Coast, China. *Mar. Geol.* **2016**, *371*, 1–17. [CrossRef]
50. Xiong, Y.; Yang, J.; Jiang, T.; Liu, H.B.; Zhong, X.M.; Tang, J.H. Early life history of the small yellow croaker (*Larimichthys polyactis*) in sandy ridges of the South Yellow Sea. *Mar. Biol. Res.* **2017**, *13*, 993–1002. [CrossRef]
51. Wu, W.F.; Zhai, F.G.; Liu, Z.Z.; Liu, C.; Gu, Y.Z.; Li, P.L. The spatial and seasonal variability of nutrient status in the seaward rivers of China shaped by the human activities. *Ecol. Indic.* **2023**, *157*, 111223. [CrossRef]
52. Yamamoto, A.; Hajima, T.; Yamazaki, D.; Aita, M.N.; Ito, A.; Kawamiya, M. Competing and accelerating effects of anthropogenic nutrient inputs on climate-driven changes in ocean carbon and oxygen cycles. *Sci. Adv.* **2022**, *8*, eabl9207. [CrossRef]
53. Santos, I.R.; Chen, X.G.; Lecher, A.L.; Sawyer, A.H.; Moosdorf, N.; Rodellas, V.; Tamborski, J.; Cho, H.M.; Dimova, N.; Sugimoto, R.; et al. Submarine groundwater discharge impacts on coastal nutrient biogeochemistry. *Nat. Rev. Earth Environ.* **2021**, *2*, 307–323. [CrossRef]
54. Zhou, Y.P.; Yang, X.; Wang, Y.; Li, F.F.; Wang, J.T.; Tan, L.J. Exogenous nutrient inputs restructure phytoplankton community and ecological stoichiometry of Eastern Indian Ocean. *Ecol. Indic.* **2021**, *127*, 107801. [CrossRef]
55. Polte, P.; Kotterba, P.; Moll, D.; von Nordheim, L. Ontogenetic loops in habitat use highlight the importance of littoral habitats for early life-stages of oceanic fishes in temperate waters. *Sci. Rep.* **2017**, *7*, 42709. [CrossRef] [PubMed]
56. Galaiduk, R.; Radford, B.T.; Saunders, B.J.; Newman, S.J.; Harvey, E.S. Characterizing ontogenetic habitat shifts in marine fishes: Advancing nascent methods for marine spatial management. *Ecol. Appl.* **2017**, *27*, 1776–1788. [CrossRef]
57. Komyakova, V.; Munday, E.L.; Jones, G.P. Comparative analysis of habitat use and ontogenetic habitat-shifts among coral reef damselfishes. *Environ. Biol. Fish.* **2019**, *102*, 1201–1218. [CrossRef]
58. Félix-Hackradt, F.C.; Hackradt, C.W.; Treviño-Otón, J.; Pérez-Ruzafa, A.; García-Charton, J.A. Habitat use and ontogenetic shifts of fish life stages at rocky reefs in South-western Mediterranean Sea. *J. Sea Res.* **2014**, *88*, 67–77. [CrossRef]
59. Drake, P.; Arias, A.M. Composition and seasonal fluctuations of the ichthyoplankton community in a shallow tidal channel of Cadiz Bay (S.W. Spain). *J. Fish Biol.* **1991**, *39*, 245–263. [CrossRef]
60. Leggett, W.C. Fish Migrations in Coastal and Estuarine Environments: A Call for New Approaches to the Study of an Old Problem. In *Mechanisms of Migration in Fishes*; NATO Conference Series; Springer: Boston, MA, USA, 1984; Volume 14.
61. Pankhurst, N.W.; Munday, P.L. Effects of climate change on fish reproduction and early life history stages. *Mar. Freshw. Res.* **2011**, *62*, 1015–1026. [CrossRef]
62. Asch, R. Climate change and decadal shifts in the phenology of larval fishes in the California Current ecosystem. *Proc. Natl. Acad. Sci. USA* **2015**, *112*, E4065–E4074. [CrossRef]
63. Kumar, P.; Babita, M.; Kailasam, M.; Muralidhar, M.; Hussain, T.; Behera, A.; Jithendran, K.P. Effect of Changing Environmental Factors on Reproductive Cycle and Endocrinology of Fishes. In *Outlook of Climate Change and Fish Nutrition*; Springer: Singapore, 2022.
64. Fincham, J.I.; Rijnsdorp, A.D.; Engelhard, G.H. Shifts in the timing of spawning in sole linked to warming sea temperatures. *J. Sea Res.* **2013**, *75*, 69–76. [CrossRef]
65. Sparks, M.M.; Westley, P.A.H.; Falke, J.A.; Quinn, T.P. Thermal adaptation and phenotypic plasticity in a warming world: Insights from common garden experiments on Alaskan sockeye salmon. *Glob. Chang. Biol.* **2017**, *23*, 5203–5217. [CrossRef]
66. Beer, W.N.; Anderson, J.J. Effect of spawning day and temperature on salmon emergence: Interpretations of a growth model for Methow River chinook. *Can. J. Fish. Aquat. Sci.* **2001**, *58*, 943–949. [CrossRef]
67. Wilson, S.M.; Moore, J.W.; Ward, E.J.; Kinsel, C.W.; Anderson, J.H.; Buehrens, T.W.; Carr-Harris, C.N.; Cochran, P.C.; Davies, T.D.; Downen, M.R.; et al. Phenological shifts and mismatch with marine productivity vary among Pacific salmon species and populations. *Nat. Ecol. Evol.* **2023**, *7*, 852–861. [CrossRef]
68. Nati, J.J.H.; Svendsen, M.B.S.; Marras, S.; Killen, S.S.; Steffensen, J.F.; McKenzie, D.J.; Domenici, P. Intraspecific variation in thermal tolerance differs between tropical and temperate fishes. *Sci. Rep.* **2021**, *11*, 21272. [CrossRef]
69. Wang, H.Y.; Shen, S.F.; Chen, Y.S.; Kiang, Y.K.; Heino, M. Life histories determine divergent population trends for fishes under climate warming. *Nat. Commun.* **2020**, *11*, 4088. [CrossRef]
70. Audzijonyte, A.; Richards, S.A.; Stuart-Smith, R.D.; Pecl, G.; Edgar, G.J.; Barrett, N.S.; Payne, N.; Blanchard, J.L. Fish body sizes change with temperature but not all species shrink with warming. *Nat. Ecol. Evol.* **2020**, *4*, 809–814. [CrossRef] [PubMed]
71. Geburzi, J.C.; McCarthy, M.L. How Do They Do It?–Understanding the Success of Marine Invasive Species. In *YOUMARES 8–Oceans Across Boundaries: Learning from Each Other*; Springer: Cham, Switzerland, 2018.

72. Ye, G.Q.; Lin, Y.; Feng, C.C.; Chou, L.M.; Jiang, Q.T.; Ma, P.P.; Yang, S.Y.; Shi, X.F.; Chen, M.R.; Yang, X.C.; et al. Could the wild population of Large Yellow Croaker *Larimichthys crocea* (Richardson) in China be restored? A case study in Guanjingyang, Fujian, China. *Aquat. Living Resour.* **2020**, *33*, 24. [CrossRef]
73. Wang, Y.; Zhou, X.J.; Chen, J.J.; Xie, B.; Huang, L.F. Climate-induced habitat suitability changes intensify fishing impacts on the life history of large yellow croaker (*Larimichthys crocea*). *Ecol. Evol.* **2022**, *12*, e9342. [CrossRef] [PubMed]
74. Sasaki, M.C.; Cheng, B.S. Populations adapt more to temperature in the ocean than on land. *Nat. Clim. Chang.* **2022**, *12*, 1098–1099.
75. Swadling, D.S.; Knott, N.A.; Taylor, M.D.; Rees, M.J.; Cadiou, G.; Davis, A.R. Consequences of Juvenile Fish Movement and Seascape Connectivity: Does the Concept of Nursery Habitat Need a Rethink? *Estuaries Coast.* **2024**, *47*, 607–621. [CrossRef]
76. Sheaves, M.; Baker, R.; Nagelkerken, I.; Connolly, R.M. True Value of Estuarine and Coastal Nurseries for Fish: Incorporating Complexity and Dynamics. *Estuaries Coast.* **2015**, *38*, 401–414. [CrossRef]
77. Takahashi, I.; Azuma, K.; Fujita, S.; Kinoshita, I. Habitat shift of ayu *Plecoglossus altivelis altivelis* in early stages from waters adjacent to the bank to the center of flow in the Shimanto Estuary. *Fish. Sci.* **2002**, *68*, 554–559. [CrossRef]
78. Hogan, J.D.; Kozdon, R.; Blum, M.J.; Gilliam, J.F.; Valley, J.W.; McIntyre, P.B. Reconstructing larval growth and habitat use in an amphidromous goby using otolith increments and microchemistry. *J. Fish Biol.* **2017**, *90*, 1338–1355. [CrossRef]
79. Sagoe, A.A.; Aheto, D.W.; Okyere, I.; Adade, R.; Odoi, J. Community participation in assessment of fisheries related ecosystem services towards the establishment of marine protected area in the Greater Cape Three Points area in Ghana. *Mar. Policy* **2020**, *124*, 104336. [CrossRef]
80. Chen, X.; Xu, Z.H.; Ding, Y.F. Jiangsu Haizhou Bay Marine Farm Construction Present Situation and Development Countermeasures and Suggestions. *China Resour. Compr. Util.* **2016**, *34*, 43–45.
81. Fu, X.M.; Wu, W.Q.; Zhang, S. Evaluation of ecological restoration performance in Haizhou Bay, Lianyungang. *J. Dalian Ocean Univ.* **2017**, *32*, 93–98.
82. Neilson, J.D.; Perry, R.I. Diel Vertical Migrations of Marine Fishes: An Obligate or Facultative Process? In *Advances in Marine Biology*; Academic Press: Pittsburgh, PA, USA, 1990.
83. Hawes, S.; Miskiewicz, T.; Garcia, V.; Figueira, W. Size and stage-dependent vertical migration patterns in reef-associated fish larvae off the eastern coast of Australia. *Deep-Sea Res. Part I* **2020**, *164*, 103362. [CrossRef]
84. Liu, Y.B.; Song, C.L.; Yang, X.; Zhuo, H.H.; Zhou, Z.; Cao, L.; Cao, X.Y.; Zhou, Y.Y.; Xu, J.; Wan, L.L. Hydrological regimes and water quality variations in the Yangtze River basin from 1998 to 2018. *Water Res.* **2023**, *249*, 120910. [CrossRef]
85. Yang, S.L.; Xu, K.H.; Milliman, J.D.; Yang, H.F.; Wu, C.S. Decline of Yangtze River water and sediment discharge: Impact from natural and anthropogenic changes. *Sci. Rep.* **2015**, *5*, 12581. [CrossRef]